SF2A 2023
M. N'Diaye, A. Siebert, N. Lagarde, O. Venot, K. Baillié, M. Béthermin, E. Lagadec, J. Malzac, J. Richard (eds)

JWST PROBES THE ROLE OF STELLAR MASS AND MORPHOLOGY IN OBSCURING GALAXIES

C. Gómez-Guijarro[1]

Abstract. In the last years a population of galaxies missed in optical surveys but bright at far-infrared/millimeter wavelengths has been discovered. These optically dark/faint galaxies (OFGs, among other nomenclatures) are of great interest as they are seen as a key population of galaxies that dominate the contribution of massive ($M_* > 10^{10.3}\,M_\odot$) galaxies to the star formation rate density of the universe at $z > 3$. However, their high-redshift, massive nature, and the reason behind their elusiveness are still uncertain. We present a *JWST*-based study investigating the drivers of dust attenuation in massive galaxies in the *JWST* era, focusing on understanding what is the nature of these OFGs that resulted in missing them in the pre-*JWST* observations. Stellar mass appears as the primary proxy of dust attenuation among those studied. However, there is a subset of highly dust attenuated ($A_V > 1$, typically) star-forming galaxies (SFGs), of which OFGs are a specific case. For this subset, we find that the key distinctive feature is their compact size. OFGs are dark because their dust content is associated to more compact stellar profiles, when compared to similarly massive SFGs at the same epoch.

Keywords: galaxies: evolution – galaxies: high-redshift – galaxies: photometry – galaxies: star formation – galaxies: structure – infrared: galaxies

1 Introduction

Prior the *JWST*, our insights into the early cosmic history of galaxies, especially those with $z > 3$, largely depended on samples chosen from their rest-frame ultraviolet (UV) light (see Madau & Dickinson 2014, for a review). Traditional selection methods, like those for Lyman break galaxies (LBGs) (LBGs; e.g., Steidel et al. 1996), often overlooked redder dusty star-forming galaxies (SFGs). Recent observations from the Spitzer Space Telescope (*Spitzer*) and the Atacama Large Millimeter/submillimeter Array (ALMA) revealed a subset of massive dusty SFGs not captured in previous optical/near-infrared (IR) surveys (e.g., Franco et al. 2018; Wang et al. 2019; Gómez-Guijarro et al. 2022). These galaxies differ from extreme dusty starbursts and are believed to play a significant role in the star-forming rate density of the universe around $z \sim 3$–6. Their precise role and characteristics, especially in terms of stellar morphologies, have been hard to uncover due to their faintness in optical/near-IR wavelengths.

With the *JWST*, light has been shed on these elusive galaxies, revealing diverse properties across multiple studies (e.g., Barrufet et al. 2022; Nelson et al. 2023; Pérez-González et al. 2023). In our study, we delve into the factors influencing dust attenuation in the *JWST* epoch, striving to discern the nature of these obscured galaxies and to elucidate why they remained elusive in the pre-*JWST* era. We emphasize the impact of stellar mass and morphology as proxies of dust attenuation and outline our methods and findings in the subsequent sections.

In this text the main results from Gómez-Guijarro et al. (2023) are outlined, to which the reader is referred for further details.

[1] Université Paris-Saclay, Université Paris Cité, CEA, CNRS, AIM, 91191, Gif-sur-Yvette, France

2 Methodology

2.1 Data and catalog

We utilized data from the *JWST*, specifically from the Cosmic Evolution Early Released Science (CEERS) survey in the Extended Groth Strip (EGS) field (Finkelstein et al. 2022), along with complementary data from the Hubble Space Telescope (*HST*) and ground-based imaging from the Canada-France-Hawaii Telescope (CFHT). For cataloging, source detection was conducted using `SExtractor` in the F444W-band, following procedures similar to the CANDELS catalog in the EGS field (Stefanon et al. 2017). Photometry was carried out across 13 *JWST* and *HST* bands using dual image mode in `SExtractor`, and on five ground-based CFHT bands using aperture photometry.

2.2 Estimation of redshift, stellar mass, dust attenuation, and morphology

We used the `EAZy` code to calculate photometric redshifts from spectral energy distribution (SED) fitting across 18 bands in our catalog, utilizing the Flexible Stellar Population Synthesis (FSPS) templates. Where high-quality spectroscopic redshifts were available, we replaced the photometric redshifts, and used them to refine the zero point corrections iteratively in the `EAZy-py` run, improving photometric redshift accuracy.

For estimating stellar masses and dust attenuation, we used the `FAST++` SED fitting code, keeping the redshifts fixed at the previously obtained values. The used stellar population models, star formation histories, and metallicity values are standard in similar studies, facilitating comparisons.

Star formation rate (SFR) values were derived from a ladder of SFR estimators. We initially checked for counterparts in mid-IR-to-mm bands. For galaxies with significant signal in the IR, we applied the `CIGALE` code to dust emission templates to derive total IR luminosity estimates. For other cases, we re-normalized IR templates to *Spitzer*/MIPS 24 μm fluxes, or used the UV term alone corrected for dust attenuation to estimate the total SFR, depending on the available data. The SFR takes into account both obscured and unobscured star formation, combining IR and UV luminosity contributions.

For morphological analysis, we employed the `statmorph` code to fit surface brightness profiles to *JWST*/NIRCam F444W images. This band was chosen as it reliably probes optical-to-near-IR rest-frame morphologies across our redshift range of interest, minimizing morphological variances observed at shorter wavelengths. Our analysis was confined to good fit quality cases to ensure reliable morphological measurements.

2.3 Sample definitions

In this, we used a selective redshift range of $3 < z < 7.5$ to incorporate insights from the *JWST*/NIRCam into the rest-frame UV analysis, with the lower limit enabling coverage of the rest-frame UV at all redshifts using at least two NIRCam bands. The study also sets a stellar mass lower limit of $\log(M_*/M_\odot) \geq 9.0$ to focus on intermediate-to-massive galaxies. Three distinct galaxy samples were classified: SFGs, LBGs, and OFGs:

Star-Forming Galaxies (SFGs) parent sample: Identified within the defined redshift and stellar mass limits using a UVJ classification (e.g., Williams et al. 2009), yielding a total of 1490 galaxies. This parent sample aimed to serve as a benchmark for comparative analysis.

Lyman Break Galaxies (LBGs): Recognized by their prominent break beyond the Lyman limit due to intervening hydrogen absorption, facilitating the identification of high-redshift SFGs. The LBGs sample encapsulated 1182 galaxies, applying specific color criteria (Bouwens et al. 2015) to identify them within the parent SFGs sample.

Optically Dark/Faint Galaxies (OFGs): Defined by their intrinsic faintness in optical/near-IR wavelengths, yet bright at longer near-IR bands, with a total of 35 galaxies classified under this category. Using specific magnitude cuts (Xiao et al. 2023), this sample exposed a complementary selection of bright galaxies, missed by the LBG criteria.

3 Results

We explored the stellar and morphological characteristics of the parent sample of SFGs, LBGs, and OFGs. We find that while all galaxy samples share similar redshift distributions, OFGs are notably more massive and dust-attenuated. Morphologically, a distribution around smaller effective radii was observed in OFGs (Fig. 1).

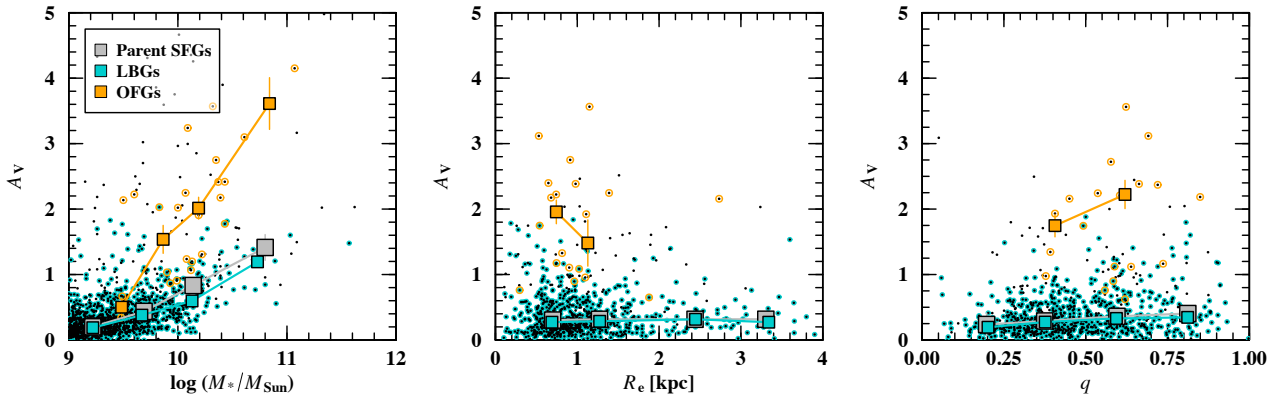

Fig. 1. From Gómez-Guijarro et al. (2023). Dust attenuation as a function of stellar mass, (circularized) effective radius, and axis ratio. Sliding medians for the different galaxy types shown in the legend are displayed with colored squares.

3.1 Drivers of dust attenuation

We investigated the impact of stellar mass and morphology on dust attenuation, particularly focusing on highly dust-attenuated galaxies like OFGs (Fig. 1). Stellar mass shows a correlation with dust attenuation in SFGs, establishing a general trend (see also e.g., Garn & Best 2010; Zahid et al. 2013; Pannella et al. 2015), with OFGs indicating a steeper trend towards a higher dust attenuation regime. This correlation stems from the mass-metallicity relation (e.g., Tremonti et al. 2004), where massive SFGs retain metals more efficiently, making them dustier compared to low mass SFGs. However, when it comes to morphology, the correlation is not as pronounced. In the case of OFGs, we find that the effective radii are generally smaller and associated with higher dust attenuation values, but no significant increase in dust attenuation is observed with lower axis ratios (edge-on galaxies). Our analysis reveals that at a common redshift and stellar mass, the $A_V > 1$ and OFGs samples are notably smaller than the parent sample of SFGs, $\sim 30\%$ smaller efective radius (Fig. 2).

The results highlight stellar mass as a key indicator of dust attenuation, while the effective radius and axis ratio do not exhibit a significant role, generally. However, among massive galaxies at similar redshifts, those with higher dust attenuation tend to have more compact stellar light profiles. To validate these observations, a Random Forest analysis was conducted (see e.g., Bluck et al. 2022, for a similar analysis). The Random Forest, a machine learning technique, aids in pinpointing the dominant parameter influencing a specified quantity, especially amidst inter-correlated parameters. This analysis was executed by segregating a target quantity and the associated features, further splitting them into training and testing samples for model training and validation respectively. Our investigation, utilizing a random forest regressor, aimed to identify the most predictive parameter of dust attenuation (A_V) among stellar mass (M_*), SFR, effective radius (R_e), and axis ratio (q). Stellar mass emerged as the most predictive parameter followed by SFR, aligning with our initial findings. Meanwhile, the morphological parameters effective radius and axis ratio did not stand out as strong predictors for dust attenuation, thereby reaffirming the observations made earlier (Fig. 2).

4 Discussion and conclusions

The findings of this work highlight the prominence of stellar mass in predicting dust attenuation. As stellar mass encapsulates a galaxy star formation history, and consequently its metal and dust composition, it plays a pivotal role in understanding dust attenuation. The data reveals that in addition to stellar mass, SFR also serves as a substantial predictor for dust attenuation.

When examining the role of orientation, it is observed that inclination holds minimal role in affecting dust attenuation at $z > 3$, close to a random variable, contrary to previous interpretations linking higher dust attenuation levels to edge-on disk galaxies (Nelson et al. 2023). The findings suggest a transition, where at such redshifts, dust attenuation is primarily governed by dust within dense star-forming regions as opposed to dust in the diffuse ISM, rendering inclination effects negligible (Lorenz et al. 2023).

Distinctly, a subset of galaxies dubbed OFGs, despite similar stellar mass, SFR, and redshift, exhibit fainter

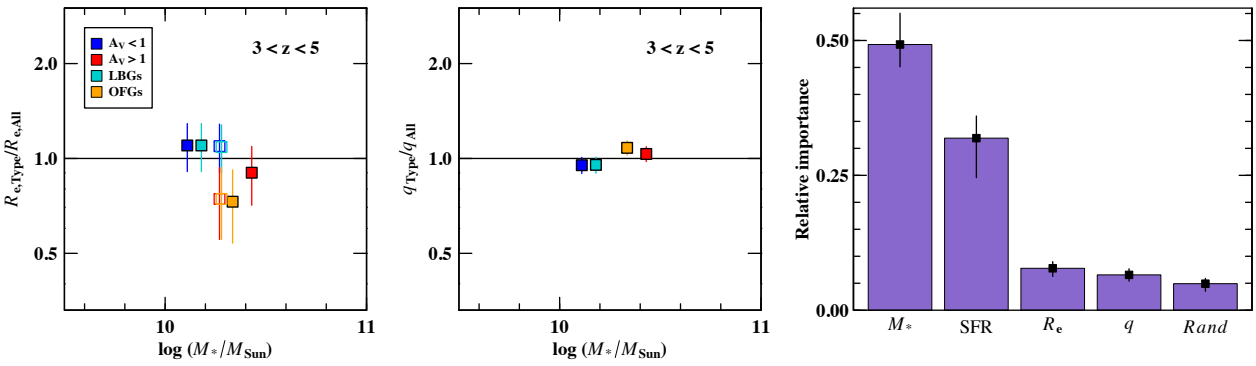

Fig. 2. From Gómez-Guijarro et al. (2023). **Left panel**: Ratio of the (circularized) effective radius for different galaxy types over those of the parent SFGs sample. Ratios after applying a correction to a common redshift and stellar mass are displayed with open squares. **Right panel**: Same as left panel for the axis ratio.

UV light, indicative of higher dust attenuation. The defining trait of these galaxies is their compact size, characterized by smaller effective radii when consider against the broader SFGs population. This compactness points to a denser distribution of their stellar profiles, which in turn, might aid in retaining metals and dust more efficiently. Moreover, the compactness of OFGs mirrors that of quiescent galaxies (QGs), suggesting a possible evolutionary linkage between the two. The condensed stellar light profiles of OFGs, coupled with their elevated SFR surface densities, echo a step towards the progressive buildup of compact QGs stellar profiles. This ties into broader galaxy evolution narratives (e.g., Barro et al. 2013; Toft et al. 2014; Gómez-Guijarro et al. 2018), hinting at the potential of OFGs serving as progenitors to massive compact QGs.

This work was carried out in collaboration with the CEERS team. CGG acknowledges support from CNES.

References

Barro, G., Faber, S. M., Pérez-González, P. G., et al. 2013, ApJ, 765, 104
Barrufet, L., Oesch, P. A., Weibel, A., et al. 2022, arXiv e-prints, arXiv:2207.14733
Bluck, A. F. L., Maiolino, R., Brownson, S., et al. 2022, A&A, 659, A160
Bouwens, R. J., Illingworth, G. D., Oesch, P. A., et al. 2015, ApJ, 803, 34
Finkelstein, S. L., Bagley, M. B., Arrabal Haro, P., et al. 2022, ApJ, 940, L55
Franco, M., Elbaz, D., Béthermin, M., et al. 2018, A&A, 620, A152
Garn, T. & Best, P. N. 2010, MNRAS, 409, 421
Gómez-Guijarro, C., Elbaz, D., Xiao, M., et al. 2022, A&A, 658, A43
Gómez-Guijarro, C., Magnelli, B., Elbaz, D., et al. 2023, A&A, 677, A34
Gómez-Guijarro, C., Toft, S., Karim, A., et al. 2018, ApJ, 856, 121
Lorenz, B., Kriek, M., Shapley, A. E., et al. 2023, arXiv e-prints, arXiv:2304.08521
Madau, P. & Dickinson, M. 2014, ARA&A, 52, 415
Nelson, E. J., Suess, K. A., Bezanson, R., et al. 2023, ApJ, 948, L18
Pannella, M., Elbaz, D., Daddi, E., et al. 2015, ApJ, 807, 141
Pérez-González, P. G., Barro, G., Annunziatella, M., et al. 2023, ApJ, 946, L16
Stefanon, M., Yan, H., Mobasher, B., et al. 2017, ApJS, 229, 32
Steidel, C. C., Giavalisco, M., Pettini, M., Dickinson, M., & Adelberger, K. L. 1996, ApJ, 462, L17
Toft, S., Smolčić, V., Magnelli, B., et al. 2014, ApJ, 782, 68
Tremonti, C. A., Heckman, T. M., Kauffmann, G., et al. 2004, ApJ, 613, 898
Wang, T., Schreiber, C., Elbaz, D., et al. 2019, Nature, 572, 211
Williams, R. J., Quadri, R. F., Franx, M., van Dokkum, P., & Labbé, I. 2009, ApJ, 691, 1879
Xiao, M. Y., Elbaz, D., Gómez-Guijarro, C., et al. 2023, A&A, 672, A18
Zahid, H. J., Yates, R. M., Kewley, L. J., & Kudritzki, R. P. 2013, ApJ, 763, 92